

Partial Domain Adaptation without Domain Alignment

Weikai Li and Songcan Chen

Abstract—Unsupervised domain adaptation (UDA) aims to transfer knowledge from a well-labeled source domain to a different but related unlabeled target domain with identical label space. Currently, the main workhorse for solving UDA is domain alignment, which has proven successful. However, it is often difficult to find an appropriate source domain with identical label space. A more practical scenario is so-called partial domain adaptation (PDA) in which the source label set or space subsumes the target one. Unfortunately, in PDA, due to the existence of the irrelevant categories in source domain, it is quite hard to obtain a perfect alignment, thus resulting in mode collapse and negative transfer. Although several efforts have been made by down-weighting the irrelevant source categories, the strategies used tend to be burdensome and risky since exactly which irrelevant categories are unknown. These challenges motivate us to find a relatively simpler alternative to solve PDA. To achieve this, we first provide a thorough theoretical analysis, which illustrates that the target risk is bounded by both model smoothness and between-domain discrepancy. Considering the difficulty of perfect alignment in solving PDA, we turn to focus on the model smoothness while discard the riskier domain alignment to enhance the adaptability of the model. Specifically, we instantiate the model smoothness as a quite simple intra-domain structure preserving (IDSP). To our best knowledge, this is the first naive attempt to address the PDA without domain alignment. Finally, our empirical results on multiple benchmark datasets demonstrate that IDSP is not only superior to the PDA SOTAs by a significant margin on some benchmarks (e.g., $\sim+10\%$ on $CI \rightarrow Rw$ and $\sim+8\%$ on $Ar \rightarrow Rw$), but also complementary to domain alignment in the standard UDA.

Index Terms—Partial Domain Adaptation, Structure Preserving, Semi-supervised Learning, manifold Learning

1 INTRODUCTION

CURRENTLY, unsupervised domain adaptation (UDA) has caught tremendous attention in the machine learning community, which learns a classifier for the unlabeled target domain by using a labeled source domain. Most existing works assume that the source and target domains share an identical label set or space [1], [2]. In this specific context, domain alignment comes to the main hotspot for solving UDA, i.e., instance re-weighting [3], feature alignment [4], [5], [6] or model adaptation [7], [8], [9]. However, in practice, it tends to be extremely burdensome and quite difficult to find an ideal source domain with identical label space [10]. In contrast, in the context of big data, a more practical alternative is to access a large-scale source domain while working on a relative small-scale target domain to cover the target label space, which is also known as the partial domain adaptation (PDA) [11], [12], [13], [14], [15], [16]. Unfortunately, in such a scenario, the conventional domain alignment often fails as a result of the irrelevant source sub-classes can be mixed with target data, resulting in mode collapse and negative transfer [13].

To alleviate this issue, almost all existing PDA studies focus on diminishing the negative impact of irrelevant source categories between two domains by an elaborately designed reweighting approach and in turn learning the domain invariant model/representation in the shared label space [11], [12], [16], [17]. Unfortunately, from an algorithmic

perspective, such an additional reweighting approach can be quite risky, since exactly which irrelevant categories are unknown. Moreover, these approaches highly rely on the pseudo labels of target domain. However, the target samples might be wrongly predicted into the irrelevant categories in the beginning under the domain shift, as shown in Fig. 1 (b) [18], [19], [20], [21], [22], making it hard to obtain a perfect alignment. The experimental results of these methods also confirm that it is difficult to accurately identify the irrelevant categories [11], [12], [17] in source domain. Further, even if the irrelevant source categories are correctly filtered, it is still hard to obtain a perfect alignment to guarantee that the target domain can be labeled correctly [22], [23], as shown in Fig. 1 (c). From a theoretical perspective, several recently proposed theoretical works reveal that the domain alignment hurts the transfer-ability of representations/model [21], [22]. Consequently, these drawbacks push us to seek an alternative for solving PDA without domain alignment.

Recently, several efforts have indeed been dedicated to addressing UDA without domain alignment, even if the domains involved share the same label set. For example, Li et al, progressively anchors the target samples and in turn refine the shared subspace for knowledge transfer [19]. Li et al, optimizes the predictive behavior in the target domain to address UDA [23]. Liu et al, enforces the pseudo labels to generalize across domains [18]. As one proverb goes, “the lesser of the two evils”, discarding the domain alignment is sometimes a wise choice when induced misalignment does more harm than good as validated by these works. Nonetheless, to the best of our knowledge, so far, there has been no attempt to address PDA without domain alignment, where the misalignment more likely occurs. At the same time, the theoretical aspect of how to transfer knowledge

- The authors are with College of Computer Science and Technology, Nanjing University of Aeronautics and Astronautics of (NUAA), Nanjing, 211106, China.
E-mail: {leeveikai; s.chen}@nuaa.edu.cn.
- Corresponding author is Songcan Chen.

Manuscript received April 19, XXXX; revised August 26, XXXX.

without domain alignment has not been well studied yet.

To address these issues, we derive a novel generalization error bound for domain adaptation which combines the model smoothness and the between-domain discrepancy. Considering both the difficulty of perfect alignment and the risk of misalignment in solving PDA, we simply bypass the domain alignment and focus on the model smoothness, which guides us to optimize the target label to have a smooth structure. Specifically, as a proof of concept, this paper presents a quite simple PDA framework to encourage the adaptation ability of the model, which instantiates the model smoothness as a commonly-used manifold structure preserving [9], [24]. In contrast to the conventional domain alignment which indirectly learns a domain invariant representation/model for adaptation, we directly optimize the target labels to enhance the adaptation performance of the model. Doing so is also quite consistent with Vapnik’s philosophy, i.e., any desired problem should be solved in a direct way [25].

Furthermore, on amount of the existence of the domain shift, the manifold structure tends to vary sharply across domains. For example, several source-private samples can be located near the target samples, and some of the source samples with common labels can be far away from the target samples as shown in Fig. 1 (e). Also, the structure information of the irrelevant categories in the source domain easily incorporate bias in learning the classifier. Thus, it can be quite perilous to leverage the structure knowledge across domains. To this end, we only consider the intra domain structure preserving (IDSP) to constrain the classifier on the target domain to alleviate the negative transfer caused by the domain gap as shown in Fig. 1 (f).

Notably, from both theoretical and empirical views, IDSP and domain alignment can complement each other, when ideal alignment is relatively easy to be conducted, especially in UDA. In addition, we would like to emphasize that the IDSP also can work well in solving UDA compared to the existing PDA methods. For facilitating efforts to replicate our results, our implementation is available on GitHub¹. In summary, this work makes the following contributions:

- A novel generalization error bound is derived, which provides an alternative (i.e., model smoothness) for solving PDA;
- A simple yet effective PDA method by intra-domain structure preserving (IDSP) is proposed, which is the first attempt, to our best knowledge, to address PDA without domain alignment;
- The experimental results reveal that the proposed IDSP can effectively enhance the adaptation ability of the model, which additionally provides an effective benchmark for PDA;
- The IDSP can be complementary to domain alignment in UDA, when domain alignment is relatively less risky in such a setting, which again tells the need of targeting at a safe transfer of knowledge.

The rest of this paper is organized as follows. In Section 2, we briefly overview UDA and PDA. In Section 3, we elaborate on the problem formulation, and provide a novel generalization error bound for domain adaptation. In Section

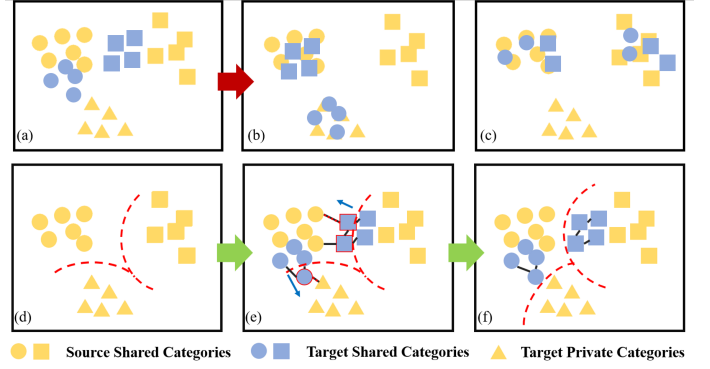


Fig. 1. Motivation of IDSP. (a) Partial domain adaptation, in which the label set or space of the source domain subsumes the target one. (b) It is risky to down weight the irrelevant categories. (c) The target samples might be wrongly predicted even if the irrelevant categories are filtered. (d) Classifier learned from the source domain. (e) The manifold structure across domains tends to vary sharply due to the domain shift. (f) We only use the intra-domain structure preserving to enhance the ability of the adaptation ability of the classifier.

4, we present the IDSP model and optimization algorithm in detail. In Section 5, we present the experimental results and the corresponding analysis. In the end, we conclude the entire paper with future research directions in Section 6

2 RELATED WORKS

In this section, we present the most related research on UDA/PDA and highlight the differences between them and our method.

2.1 Unsupervised Domain Adaptation

Recent practices on UDA usually attempt to minimize the domain discrepancy for borrowing the existing well-established source domain knowledge. Following this, multiple domain adaptation techniques have been developed, including instance re-weighting [3], [26], [27], feature alignment [4], [5], [6] and classifier adaptation [7], [8], [9]. The instance re-weighting methods focus on correcting the distribution biases in the data sampling procedure through reweighting the individual samples to minimize the \mathcal{A} -distance [27], Maximum Mean Discrepancy (MMD) [3], or KL-divergence [26]. The feature alignment methods generate the domain-invariant feature to reduce the distribution differences across domains, such as MMD [4], Central Moment Discrepancy [28], Bregman divergence [29], Joint MMD [7], [30], \mathcal{A} -distance [6], Maximum Classifier Discrepancy [31], Wasserstein distance [32], Δ -distance [33], or the distance between the second-order statistics (covariance) of the source and target features [34]. The classifier adaptation methods adapt the model parameter of source domain to target domain by imposing the additional constraints for alignment [7], [8], [9].

The proposed IDSP can be summarized into the classifier adaptation. However, IDSP does not align the target and source domains but uses the intra-domain structure preserving to enhance the adaptation ability of the model. In addition, all of the existing UDA methods assume the source label space and target label space are identical, which is

1. <https://github.com/Cavin-Lee/IDSP>.

often too strict to be satisfied in the real-world applications. The proposed IDSP relaxes this assumption and aims to address a more challenging PDA problem.

2.2 Partial Domain Adaptation

PDA is a more practical scenario in which the source label space submerges the target one [11]. Owing to the existence of the irrelevant categories in the source domain, the risk of mis-alignment and mode collapse is highly increased. To address such issues, the existing approaches mainly focus on mitigating the potential negative transfer caused by irrelevant classes in the source domain by class-reweighting [11], [14], [16], [35] or example-reweighting [12], [13].

Specifically, the class-reweighting works focus on alleviating the negative transfer caused by the source-private classes. To achieve this, Partial Adversarial Domain Adaptation (PADA) alleviates the negative transfer by down-weighting the data of irrelevant classes in the source domain with the guidance of domain discriminator [11]. Selective Adversarial Network (SAN) [35] extends PADA to maximally match the data distributions in the shared class space by adding multiple domain discriminators. Deep Residual Correction Network (DRCN) plugs one residual block into the source network to enhance the adaptation from source to target and explicitly weakens the influence from the irrelevant source classes [14]. Conditional and Label Shift (CLS) introduce a class-wise balancing parameter to align both marginal and conditional distribution between source and target domains [16].

In contrast to the mentioned class re-weighting scheme, Importance Weighted Adversarial Nets (IWAN) follows the idea of instance re-weighting to filter out the influence of the irrelevant samples in the source domain. Two Weighted Inconsistency-reduced Networks (TWINS) designs an inconsistency loss to down-weighting the outlier sample in the source domain [13]. Example Transfer Network (ETN) integrates the discriminative information into the sample-level weighting mechanism [12].

Almost all of the existing PDA methods rely on various adversarial strategies and deep networks to learn the target model with the guidance of the specifically designed class/sample reweighting approaches. However, such an approach could be vulnerable in terms of adaptation due to the agnostic label space. Besides, the weighted adversarial training based methods may suffer from the issues of training instability and mode collapse, since they are highly base on the unreliable pseudo labels [19]. In contrast, IDSP requires neither adversarial training nor reweighting and thus highly mitigates these issues. In addition, the IDSP does not filter out the outlier classes and thus can also work well on UDA.

3 A THEORETICAL ANALYSIS FOR DOMAIN ADAPTATION

Current theoretical works on domain adaptation encourages domain alignment in solving domain adaptation [1], [2]. Unfortunately, it is often hard to obtain an 'ideal' alignment in domain adaptation. To find a relatively simpler

alternative, we now attempt to generate a novel generalization error bound for solving domain adaptation.

3.1 Notions and Definitions

In this paper, we focus on the PDA and UDA scenarios. We use $\mathcal{X} \in \mathbb{R}^d$ and $\mathcal{Y} \in \mathbb{R}$ to denote the input and output space, respectively. The PDA and UDA scenarios constitute a labeled source domain $\mathcal{D}_s = \{x_i^s, y_i^s\}_{i=1}^n$ with n samples, and an unlabeled target domain $\mathcal{D}_t = \{x_i^t\}_{i=n+1}^{n+m}$ with m samples. Specifically, $x_i \in \mathcal{X}$ and $y_i \in \mathcal{Y}$ are the feature and label of i -th sample, respectively. The source and target domains follow the distributions \mathbb{P} and \mathbb{Q} , respectively, and $\mathbb{P} \neq \mathbb{Q}$. Let \mathcal{X}_s , \mathcal{X}_t and \mathcal{Y}_s , \mathcal{Y}_t denote the feature and label spaces of source and target domains, respectively. We assume that the source and target domains share the same feature space i.e., $\mathcal{X}_s = \mathcal{X}_t$. For PDA, the target label space \mathcal{Y}_t is submerged by the source label space \mathcal{Y}_s , i.e., $\mathcal{Y}_t \subset \mathcal{Y}_s$. Here, we further have $\mathbb{P}_s \neq \mathbb{Q}$, where \mathbb{P}_s is the distribution of the share classes in the source domain. For UDA, the source and target domains share the identical label space, i.e., $\mathcal{Y}_s = \mathcal{Y}_t$. The goal of both PDA and UDA is to transfer the discriminative information from the source domain. In addition, our generalization bounds are based on the following Total Variation distance [36] and model smoothness.

Definition 1. *Total Variation distance [36]: Given two distributions \mathbb{P} and \mathbb{Q} . The Total Variation-distance $\text{TV}(\mathbb{P}, \mathbb{Q})$ between distributions \mathbb{P} and \mathbb{Q} is defined as:*

$$\text{TV}(\mathbb{P}, \mathbb{Q}) = \frac{1}{2} \int_{\mathcal{X}} |d\mathbb{P}(\mathbf{x}) - d\mathbb{Q}(\mathbf{x})|. \quad (1)$$

Definition 2. *Model Smoothness: A model f is r -cover with ϵ smoothness on distribution \mathbb{P} , if*

$$\mathbb{E}_{\mathbb{P}} \left[\sup_{\|\delta\|_{\infty} \leq r} |f(\mathbf{w}, \mathbf{x} + \delta) - f(\mathbf{w}, \mathbf{x})| \right] \leq \epsilon. \quad (2)$$

3.2 Generalization Error Bound with Smoothness

Inspired by a recent theoretical study [37], we assume that both the source and target domains have a compact support $\mathcal{X} \in \mathbb{R}^d$. Thus, there exists $D > 0$, such that $\forall \mathbf{u}, \mathbf{v} \in \mathcal{X}, \|\mathbf{u} - \mathbf{v}\| < D$. Let $\mathcal{L}(f(\mathbf{x}), y)$ be the loss function. We represent the expected risk of model f over distribution \mathbb{P} as $\mathcal{E}_{\mathbb{P}}(f) = \mathbb{E}_{\{x, y\} \sim \mathbb{P}} \mathcal{L}(f(x), y)$. In addition, we also assume that $0 \leq \mathcal{L}(f(\mathbf{x}), y) \leq M$ for constant M without loss of generality.

Theorem 1. *Given two distributions \mathbb{P} and \mathbb{Q} , if a model f is $2r$ -cover with ϵ smoothness over distributions \mathbb{P} and \mathbb{Q} , with probability at least $1 - \theta$, we have:*

$$\begin{aligned}
\mathcal{E}_{\mathbb{Q}}(f) &\leq \mathcal{E}_{\mathbb{P}}(f) + 2\epsilon + 2M TV(\mathbb{P}, \mathbb{Q}) \\
&\quad + M \sqrt{\frac{(2d)^{\frac{2\epsilon^2 D}{r^2} + 1} \log 2 + 2 \log\left(\frac{1}{\theta}\right)}{m}} \\
&\quad + M \sqrt{\frac{(2d)^{\frac{2\epsilon^2 D}{r^2} + 1} \log 2 + 2 \log\left(\frac{1}{\theta}\right)}{n}} \\
&\quad + M \sqrt{\frac{\log(1/\theta)}{2m}}.
\end{aligned} \tag{3}$$

The proof is given in Appendix A. This generalization error bound ensures that the target risk $\mathcal{E}_{\mathbb{Q}}$ is bounded by the source risk $\mathcal{E}_{\mathbb{P}}(f)$, the model smoothness ϵ and the domain discrepancy $TV(\mathbb{P}, \mathbb{Q})$. While the misalignment tends to be risky for solving PDA, we turn to focus on decreasing the ϵ to guarantee a low target risk. In other words, if two points $x_1, x_2 \in \mathcal{X}$ are close, then the conditional distributions $P(y|x_1)$ and $P(y|x_2)$ should be similar.

4 INTRA DOMAIN STRUCTURE PRESERVING

In this section, we exploit the theoretical results introduced above to derive a simple and practical PDA algorithm for proof of concept. Specifically, we focus on model smoothness and propose an Intra Domain Structure Preserving (IDSP) regularizer to address PDA. In the following, we go through the details of IDSP.

4.1 Main Idea

Our goal is to learn an adaptive classifier for the target domain \mathcal{D}_t . To begin with, we suppose the classifier be $f = \mathbf{w}^\top \phi(\mathbf{x})$, where $\phi(\cdot)$ denotes the feature mapping function that projects the original feature space to the Hilbert space \mathcal{H} and \mathbf{w} is the parameter of the classifier. Then, we induce a standard structural risk minimization principle [38] as:

$$f = \arg \min_{f \in \mathcal{H}_K} \mathcal{L}(f(x), y) + \lambda \mathcal{R}(f), \tag{4}$$

where the first term represents the loss on data samples, which represents the empirical risk of the training data. The second term refers to the regularization term. \mathcal{H}_K is the Hilbert space induced by kernel function $K(\cdot, \cdot)$. The main idea of this paper is to incorporate an appropriate regularization term to learn a classifier f for target domain.

Specifically, we attempt to discard the domain alignment, since misalignment tends to do more harm than good in PDA [11] and even in UDA [22]. Motivated by the theoretical analysis, we turn to focus on the model smoothness. As a proof of concept, we assume that the data lies on a manifold and follow a recent study [9] to add a Laplacian regularization term to learn the model smoothness ϵ^2 .

2. Here, we emphasize that such a strategy is only a simple attempt, which means that any other model smoothness trick such as consistency regularization [39], [40] can also be adopted to solve PDA/UDA.

4.2 Learning Classifier

To learn the classifier f , we only calculate the empirical risk on the source domain, since the target domain has no label information. In addition, we adopt the most commonly-used square loss, i.e., l_2 as the empirical risk. Then, f can be represented as:

$$f = \arg \min_{f \in \mathcal{H}_K} \sum_{i=1}^n (y_i - f(\mathbf{x}_i))^2 + \lambda \|f\|_K^2. \tag{5}$$

Moreover, we incorporate an additional $\|f\|_K^2$ constraint followed by Regularized Least Squares (RLS) [41].

4.3 Intra Domain Structure Preserving

For a safe transfer of knowledge, we only focus on model smoothness and model it as the intra domain structure preserving. Specifically, as the manifold structure may vary sharply cross domains due to the domain shift and the structure information of the irrelevant categories in the source domain easily introduce bias in the learned classifier, it tends to be risky to leverage the structure information of the source domain. Thus, we only add a Laplacian regularization term on target domain to preserve its intra domain structure. In the following, we present the graph construction and Laplacian regularization of IDSP.

4.3.1 Graph Construction

The core for structure preserving is the graph construction. The pair-wise affinity matrix \mathbf{G} of the graph can be formulated as follows:

$$\hat{\mathbf{G}}_{ij} = \begin{cases} \text{sim}(\mathbf{x}_i, \mathbf{x}_j), & \mathbf{x}_i \in \mathcal{N}_p(\mathbf{x}_j) \\ 0, & \text{otherwise} \end{cases}, \tag{6}$$

where $\text{sim}(\cdot, \cdot)$ denotes a proper similarity measurement (this paper use the cosine distance) between two samples. \mathcal{N}_p represents the set of p -nearest neighbors of point \mathbf{x}_i . Since we only consider the intra domain structure preserving of target domain, we further have:

$$\mathbf{G}_{ij} = \begin{cases} \hat{\mathbf{G}}_{ij}, & \mathbf{x}_i \text{ and } \mathbf{x}_j \in \mathcal{D}_t \\ 0, & \text{otherwise} \end{cases}. \tag{7}$$

Notably, if we further have $\mathbf{G}_{ij} = \hat{\mathbf{G}}_{ij}$ where \mathbf{x}_i and $\mathbf{x}_j \in \mathcal{D}_s$, we will preserve the intra structure of both source and target domain (ST). In addition, if $\forall i, j, \mathbf{G}_{ij} = \hat{\mathbf{G}}_{ij}$, the model will degenerate to the conventional manifold structure preserving (CST).

4.3.2 Laplacian Regularization

By introducing Laplacian matrix $\mathbf{L} = \mathbf{D} - \mathbf{G}$, where $\mathbf{D}_{ii} = \sum_{j=1}^{n+m} \mathbf{G}_{ij}$ is the diagonal matrix, the Laplacian regularization $R_L(f)$ can be expressed by

$$\begin{aligned}
R_L(f) &= \sum_{i,j=1}^{n+m} (f(\mathbf{x}_i) - f(\mathbf{x}_j))^2 \mathbf{G}_{ij} \\
&= \sum_{i,j=1}^{n+m} f(\mathbf{x}_i) \mathbf{L}_{ij} f(\mathbf{x}_j).
\end{aligned} \tag{8}$$

4.4 Overall Reformulation

Substituting with equations 5 and 8 in equation 4, the overall reformulation can be reformulated as:

$$f = \arg \min_{f \in \mathcal{H}_K} \sum_{i=1}^n (y_i - f(\mathbf{x}_i))^2 + \lambda \|f\|_K^2 + \gamma \sum_{i,j=1}^{n+m} f(\mathbf{x}_i) \mathbf{L}_{ij} f(\mathbf{x}_j), \quad (9)$$

where λ and γ are regularization hyper-parameters accordingly.

4.5 Learning Algorithm

The major difficulty of the optimization lies in that the kernel mapping $\phi: \mathcal{X} \rightarrow \mathcal{H}$ may have infinite dimensions. To solve Eq. 9 effectively, we reformulate it by using the following revised Representer theorem.

Theorem 2. *Representer Theorem: The parameter $\mathbf{W}^* = [\mathbf{w}_1^*, \dots, \mathbf{w}_n^*]$ for the optimized solution f of Eq.9 can be expressed in terms of the cross-domain labeled and unlabeled examples,*

$$f(\mathbf{x}) = \sum_{i=1}^{n+m} \alpha_i K(\mathbf{x}_i, \mathbf{x}) \quad \text{and} \quad \mathbf{w} = \sum_{i=1}^{n+m} \alpha_i \phi(\mathbf{x}_i), \quad (10)$$

where K is a kernel induced by ϕ , α_i is a weighting coefficient. The proof is given in Appendix B.

By incorporating Eq.7 into Eq. 9, we obtain the following objective³:

$$\alpha = \arg \min_{\alpha \in \mathbb{R}^{n+m}} \left\| (\mathbf{Y} - \alpha^T \mathbf{K}) \mathbf{V} \right\|_F^2 + \text{tr} \left(\lambda \alpha^T \mathbf{K} \alpha + \gamma \alpha^T \mathbf{K} \mathbf{L} \mathbf{K} \alpha \right). \quad (11)$$

where \mathbf{V} is the label indicator matrix with $\mathbf{V}_{ii} = 1$ if $i \in \mathcal{D}_s$, otherwise $\mathbf{V}_{ii} = 0$. Setting derivative of objective function as 0 leads to:

$$\alpha = ((\mathbf{V} + \gamma \mathbf{L}) \mathbf{K} + \lambda \mathbf{I})^{-1} \mathbf{V} \mathbf{Y}^T. \quad (12)$$

The learning algorithms are summarized in Algorithm 1.

Algorithm 1 Learning algorithm for IDSP

Input:

- n source labeled datasets $\mathcal{D}_s = \{\mathbf{x}_i^s, y_i\}_{i=1}^n$
- m target unlabeled datasets $\mathcal{D}_t = \{\mathbf{x}_i^s\}_{i=1}^m$
- Hyper-parameters λ, γ, p ;

Output:

- Predictive Classifier f
 - 1: Calculate the graph Laplacian \mathbf{L} by Eq.(7)
 - 2: Construct kernel \mathbf{K} by a specific kernel function;
 - 3: Compute α by Eq.(12);
 - 4: Return Classifier f by Eq.(10);
-

3. We need to state that although our framework is based on kernel method, it can be easily applied to the deep model by reformulating the $\phi(x)$.

TABLE 1
Statistics of the benchmark datasets

Dataset	#Sample	#Class	#Domain
Office-Home	15500	65	Ar, Cl, Pr, Rw
Image-Clef	7200	12	C, I, P
Office-31	4652	31	A, W, D

4.6 Complexity Analysis

The computational complexity for solving IDSP consists of three parts. We denote s as the average number of non-zero features of each sample and we have $s \leq d, p \ll \min(n+m, d)$. Solving the Eq. 12 by LU decomposition requires $\mathcal{O}((n+m)^3)$. For constructing the graph Laplacian matrix \mathbf{L} , IDSP requires $\mathcal{O}(sm^2)$. For constructing the kernel matrix \mathbf{K} , IDSP requires $\mathcal{O}((n+m)^2)$. Thus, the total complexity of IDSP is $\mathcal{O}((n+m)^3 + sm^2 + (n+m)^2)$. It should be noted that it is not difficult to speed up the algorithm using conjugate gradient method [7] or kernel approximation method [42], which is beyond the scope of this work.

5 EXPERIMENTS

To evaluate the performance of IDSP, we conduct multiple experiments over both the PDA and the UDA settings on the most widely-used benchmark datasets including *Office-Home*, *Image-Clef* and *Office-31*. Table 1 lists the statistics of the three datasets.

5.1 IDSP on PDA

5.1.1 Datasets for PDA

We first evaluate the performance of IDSP on the widely-adopted PDA benchmarks, i.e., *Office-31* and *Office-Home*. The details of the datasets are given as follows:

Office-31 [43] contains 4652 images with 31 categories in three visual domains including Amazon(A), DSLR(D) and Webcam(W). For the setting of PDA, we follow the same splits used in recent PDA studies [11], [35]. Specifically, the target domains only contain 10 categories, which is shared with Caltech-256.

Office-Home is released at CVPR'17 [44], which contains 65 different objects from 4 domains including 15588 images: Artistic images (Ar), Clipart images (Cl), Product images (Pr) and Real-world images (Rw). Reference to the PDA setting in recent studies [11], [35], the first 25 categories (in alphabetical order) are taken as the target categories, while the others as the source private categories.

5.1.2 Experimental Setup

In order to evaluate the performance of IDSP on the PDA setting, we compare IDSP with several PDA SOTAs: Partial Adversarial Domain Adaptation (PADA) [11], Selective Adversarial Network (SAN) [35], Two Weighted Inconsistency-reduced Networks (TWINS) [13], Importance Weighted Adversarial Network (IWAN) [17], Example Transfer Network (ETN) [12], Deep Residual Correction Network (DRCN) [14] and Conditional and Label Shift (CLS) [16]. To illustrate the difficulty of domain alignment in solving PDA, we further

TABLE 2
Accuracy (%) on *Office-Home* for PDA from 61 classes to 25 classes

	UDA Methods					PDA Methods					
	ResNet	DAN	DANN	MEDA	PAS	PADA	DRCN	IWAN	SAN	ETN	IDSP
Ar→Cl	38.6	44.4	44.9	52.1	55.0	52.0	54.0	53.9	44.4	59.2	60.8
Ar→Pr	60.8	61.8	54.1	73.8	75.7	67.0	76.4	54.5	68.7	77.0	80.8
Ar→Rw	75.2	74.5	69.0	78.9	83.9	78.7	83.0	78.1	74.6	79.5	87.3
Cl→Ar	39.9	41.8	36.3	57.9	66.3	52.2	62.1	61.3	67.5	62.9	69.3
Cl→Pr	48.1	45.2	34.3	61.8	73.3	53.8	64.5	48.0	<u>65.0</u>	65.7	76.0
Cl→Rw	52.9	54.1	45.2	71.1	74.7	59.0	71.0	63.3	77.8	75.0	80.2
Pr→Ar	49.7	46.9	44.1	59.7	65.7	52.6	70.8	54.2	<u>59.8</u>	68.3	74.7
Pr→Cl	30.9	38.1	38.0	48.5	55.5	43.2	49.8	52.0	44.7	55.4	59.2
Pr→Rw	70.8	68.4	68.7	77.6	<u>79.4</u>	78.8	80.5	81.3	80.1	84.4	85.3
Rw→Ar	65.4	64.4	53.0	68.6	71.8	73.7	77.5	76.5	72.2	75.7	77.8
Rw→Cl	41.8	45.4	34.7	53.0	54.3	56.6	<u>59.1</u>	56.7	50.2	57.7	61.3
Rw→Pr	70.4	68.8	46.5	78.5	82.0	77.1	79.9	82.9	78.7	85.5	85.7
AVE	53.7	54.5	47.4	65.1	69.8	62.1	69.0	63.6	65.3	<u>70.5</u>	74.9

All PDA methods are achieved by the weighted domain alignment approach except IDSP, which is the same with the following Table 3. Both MEDA and IDSP incorporate the manifold regularization term. Both PAS and IDSP are the non-aligned methods. The best accuracy is presented in bold and the second best is underlined, similarly hereinafter.

TABLE 3
Accuracy (%) on *Office-31* for PDA from 31 classes to 10 classes

	UDA Methods					PDA Methods							
	ResNet	DAN	DANN	MEDA	PAS	PADA	TWINs	DRCN	IWAN	SAN	ETN	CLS	IDSP
A→W	54.5	46.4	41.4	79.3	97.0	86.5	86.0	90.8	89.2	93.9	94.5	99.6	99.7
D→W	94.6	53.6	46.8	97.0	99.3	99.3	99.3	100	99.3	99.3	100	100	99.7
W→D	94.3	58.6	38.9	<u>99.4</u>	100	100	100	<u>99.4</u>	100	100	100	100	100
A→D	65.6	42.7	41.4	<u>85.3</u>	98.4	82.2	86.8	86.0	<u>90.5</u>	82.2	95.0	97.3	99.4
D→A	73.2	65.7	41.3	92.0	94.6	92.7	94.7	95.6	95.6	92.7	<u>96.2</u>	97.9	95.1
W→A	71.7	65.3	44.7	91.6	94.4	95.4	94.5	95.8	94.3	95.4	94.6	98.3	95.7
AVE	75.6	55.4	42.4	90.7	97.2	92.7	93.6	94.3	94.7	92.7	96.7	98.2	98.3

compare several traditional learning and UDA benchmarks including ResNet [45], Manifold Embedded Distribution Alignment (MEDA) [24], Deep Adaptation Network (DAN) [46] and Domain Adversarial Neural Networks (DANN) [6]. For the non-aligned method, we only compared Progressive Adaptation of Subspaces (PAS) [19], since only PAS performed the PDA experiment in the original paper. For a fair comparison, we use the 2048-dimensional deep feature (extracted using ResNet50 pre-trained on ImageNet) for both IDSP and other shallow UDA approach (i.e., MEDA and PAS). The optimal parameters of all compared methods are set following their original papers. Note that several results are directly obtained from the published papers if we follow the same setting. As for IDSP, we empirically set the hyper-parameters $\lambda = 0.1$, $\gamma = 5$ and $p = 10$ for the PDA setting. To evaluate the performance, we follow the widely used **accuracy** as a measurement.

5.1.3 Experimental Results

The classification results of 12 PDA tasks on *Office-Home* dataset and 6 PDA tasks on *Office-31* dataset are given in Table 2 and Table 3, respectively. Specifically, on both two datasets, our approach achieves the superior results with average accuracies of 74.9% on *Office-31* dataset and 98.3% on *Office-31* dataset by using a simple laplacian regularization term. IDSP outperforms the state of the art by a significant margin on several task (+10% on Cl→Rw, +8% on Ar→Rw and +6% on Cl→Ar). In addition, IDSP achieves the best results on all 12 tasks at *Office-Home* dataset and achieves the best/second best on all 6 tasks at *Office-31* dataset. Notably,

the UDA methods (e.g., DAN, DANN) work even worse than the baseline method without DA (i.e., ResNet), the reason is that the risk of mode collapse and mis-alignment is highly increased in the PDA setting. Moreover, it should be noted that MEDA consists of both structure preserving and domain alignment, whose results have a huge gap between IDSP, which illustrates that the domain alignment tends to hurt the adaptation and causes the negative transfer in the PDA setting. Also, MEDA achieves better results than PADA in *Office-Home* dataset, which also validates the performance gain brought by the model smoothness. In addition, PAS also achieves a quite comparable results on PDA, which reveals that discarding domain alignment is a wise choice in PDA. To sum up, the results reveal the effectiveness of the IDSP for solving PDA, while perfect alignment is quite hard to obtain in PDA setting.

5.2 IDSP on UDA

5.2.1 Dataset

We also validate the performance of IDSP on the UDA setting. Two datasets including *Office-Home* and *Image-Clef* are adopted, which are both the commonly-used benchmark datasets for the closed-set UDA and widely adopted in the most existing works such as [4], [6], [30], [44], [46]. We select all categories in the *Office-Home* for the UDA setting. The statistic information of the *Image-CLEF* is given as follows.

Image-CLEF [30] derives from Image-CLEF 2014 domain adaptation challenge, and is organized by selecting 12 object

TABLE 4
Accuracy (%) on *Office-Home* for UDA with closed-set

	ResNet	1NN	TCA	TJM	CORAL	GFK	SA	DAN	DANN	JAN	CDAN	PAS	MEDA	IDSP
Ar→Cl	34.9	45.3	38.3	38.1	42.2	38.9	43.6	43.6	45.6	45.9	46.6	52.2	55.2	55.0
Ar→Pr	50.0	57.0	58.7	58.4	59.1	57.1	63.3	57.0	59.3	61.2	65.9	72.9	76.2	74.5
Ar→Rw	58.0	45.7	61.7	62.0	64.9	60.1	68.0	67.9	70.1	68.9	73.4	76.9	77.3	76.3
Cl→Ar	37.4	57.0	39.3	38.4	46.4	38.7	47.7	45.8	47.0	50.4	55.7	58.4	58.0	59.1
Cl→Pr	41.9	58.7	52.4	52.9	56.3	53.1	60.7	56.5	58.5	59.7	62.7	68.1	73.7	71.0
Cl→Rw	46.2	48.1	56.0	55.5	58.3	55.5	61.9	60.4	60.9	61.0	64.2	69.7	71.9	70.4
Pr→Ar	38.5	42.9	42.6	41.5	45.4	42.2	48.2	44.0	46.1	45.8	51.8	58.3	59.3	60.4
Pr→Cl	31.2	42.9	37.5	37.8	41.2	37.6	41.5	43.6	43.7	43.4	49.1	47.4	52.4	52.7
Pr→Rw	60.4	68.9	64.1	65.0	68.5	64.6	70.0	67.7	68.5	70.3	74.5	76.6	77.9	77.6
Rw→Ar	53.9	60.8	52.6	53.0	60.1	53.7	59.4	63.1	63.2	63.9	68.2	67.1	68.2	68.9
Rw→Cl	41.2	48.3	41.7	42.0	48.2	42.3	47.4	51.5	51.8	52.4	56.9	53.5	57.5	56.5
Rw→Pr	59.9	74.7	70.5	71.4	73.1	70.6	74.6	74.3	76.8	76.8	80.7	77.6	81.8	82.1
AVE	46.1	56.4	51.3	51.3	55.3	51.2	57.2	56.3	57.6	58.3	62.8	64.9	67.5	67.0

TABLE 5
Accuracy (%) on *Image-Clef* for UDA with closed-set

	ResNet	1NN	TCA	TJM	CORAL	GFK	SA	DAN	DANN	JAN	CDAN	PAS	MEDA	IDSP
C→I	78.0	83.5	89.3	90.0	83.0	86.3	88.2	86.3	87.0	89.5	91.3	90.5	92.7	91.2
C→P	65.5	71.3	74.5	75.0	71.5	73.3	74.3	69.2	74.3	74.2	74.2	75.5	79.1	74.7
I→C	91.5	89.0	93.2	94.2	88.7	93.0	94.5	92.8	96.2	94.7	97.7	95.1	96.2	95.7
I→P	74.8	74.8	77.5	76.2	73.7	75.5	76.8	74.5	75.0	76.8	77.7	78.3	80.2	78.5
P→C	91.2	76.2	83.7	85.3	72.0	82.3	93.5	89.8	91.5	91.7	94.3	95.5	95.8	95.7
P→I	83.9	74.0	80.8	80.3	71.3	78.0	88.3	82.2	86.0	88.0	90.7	92.0	91.5	91.5
AVE	80.7	78.1	83.2	83.5	76.7	81.4	85.9	82.5	85.0	85.8	87.7	87.8	89.3	87.9

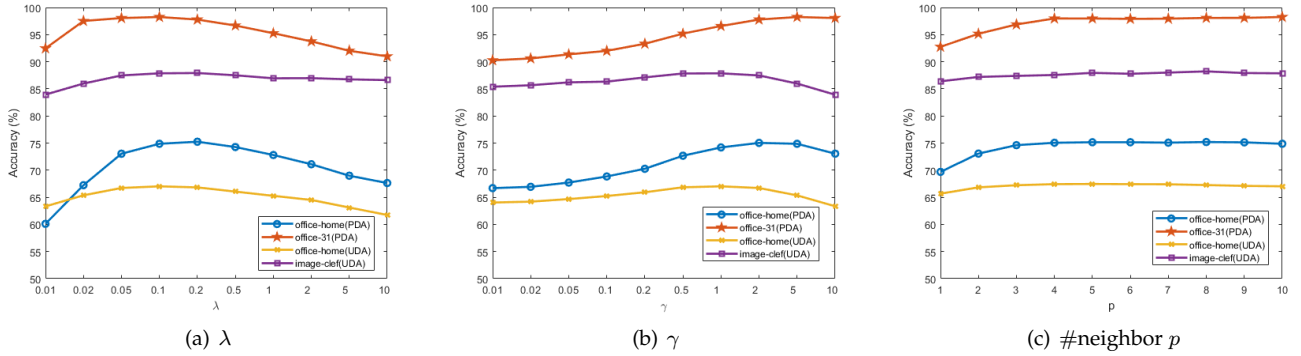


Fig. 2. classification accuracy w.r.t. p , λ and γ , respectively

categories shared in the three famous real-world datasets, ImageNet ILSVRC 2012 (I), Pascal VOC 2012 (P), Caltech-256 (C). It includes 50 images in each category and totally 600 images for each domain.

5.2.2 Experimental Setup

We compare IDSP respectively with several UDA SO-TAs: 1 Nearest Neighbor (1NN), Transfer Component Analysis (TCA) [4], Transfer Joint Matching (TJM) [7], Correlation Alignment (CORAL) [34], Geodesic Flow Kernel (GFK) [47], Subspace Alignment (SA) [5], ResNet50 [45], DAN [46], DANN [6], Joint Adaptation Networks (JAN) [30], Conditional Adversarial Networks (CDAN) [33], MEDA [24] and PAS [19]. The results of the deep-learning-based approaches (e.g., DAN, DANN, JAN and CDAN) are obtained directly from the existing works [6], [30], [33], [46]. For fair comparison, we use the 2048-dimensional deep feature

(extracted using ResNet50 pre-trained on ImageNet) for both IDSP and other shallow UDA approaches. The optimal parameters of all compared methods are set according to their original papers. As for IDSP, we empirically set the hyper-parameters $\lambda = 0.1$, $\gamma = 1$ and $p = 10$ for the UDA setting.

5.2.3 Experimental Results

The classification results of the 12 UDA tasks on *Office-Home* dataset and 6 UDA tasks on *Image-Clef* dataset are given in Table 4 and Table 5, respectively. On both two datasets, our approach achieves comparable results with average accuracy of 67.0 % on *Office-Home* dataset and 87.9% on *Image-Clef* dataset. Specifically, the IDSP achieves the best or the second-best results on 11 tasks at *Office-Home* dataset and achieves the best/second-best on 4 tasks at *Office-31* dataset. The results illustrate the effectiveness and the

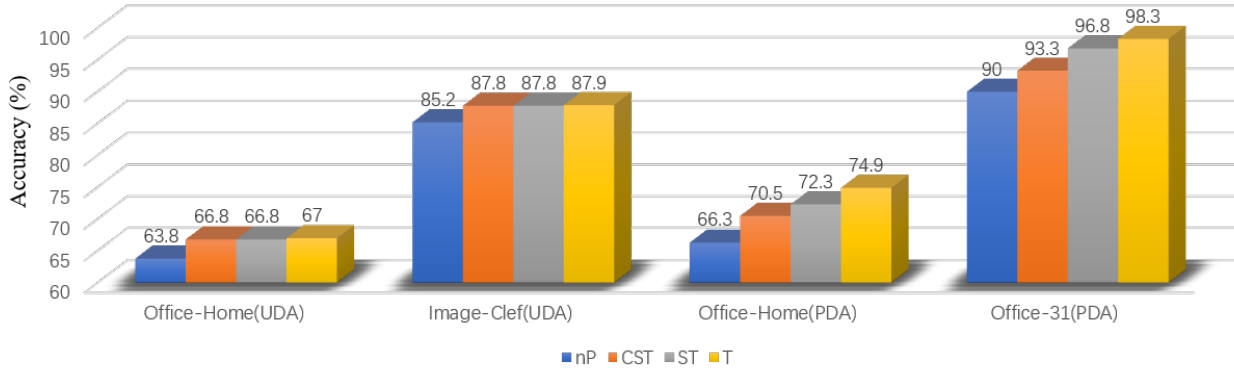


Fig. 3. Performance on UDA/PDA with different structure preserving: no structure preserving (nP), inter and intra structure of source and target domain (CST), intra structure of both source and target domain (ST) and intra structure of target domain (T)

TABLE 6
Accuracy(%) of IDSP and IDSP-JDA

DataSets	IDSP	IDSP-JDA
Office-Home(UDA)	67.0	68.0
Image-Clef(UDA)	87.9	89.3
Office-Home(PDA)	74.9	63.3
Office-31(PDA)	98.3	89.3

flexibility of model smoothness for solving UDA. Notably, MEDA incorporates both manifold and domain alignment regularization terms. The superior results of MEDA further show that model smoothness and domain alignment can complement each other since the perfect alignment tends much easier to obtain in UDA.

5.3 Joint Work with Domain Alignment

To validate the influence of domain alignment for IDSP, we further conduct experiments by adding an additional joint distribution adaptation (JDA) term [48] on UDA and PDA settings. The results are given in Table 6. As we observe, in the UDA setting, the results of (IDSP+JDA) achieve superior results with the accuracy of 68.0 % on *Office-Home* dataset and 89.3% on *Image-Clef* dataset. The results illustrate that domain alignment and IDSP can be complementary with each other at a safe transfer of knowledge. In contrast, in the PDA setting, we can find that the adaption performance will be significantly decreased if we incorporate the domain alignment. More details can be found in Appendix C. The results reveal that it is beneficial to discard domain alignment in PDA at least in more risky settings where perfect alignment is hard to be achieved.

5.4 Sensitivity Analysis

The proposed IDSP method involves three hyper-parameters (i.e., λ for l_2 -regularization, γ for laplacian regularization and neighbor p). To investigate the sensitivity of these hyper-parameters on performance, we conduct experiments on *office-Home*, *Image-Clef* and *Office-31* datasets. Specifically, we run IDSP by searching $\lambda \in \{0.01, 0.02, 0.05, 0.1, 0.2, 0.5, 1, 2, 5, 10\}$, $\gamma \in \{0.01, 0.02, 0.05, 0.1, 0.2, 0.5, 1, 2, 5, 10\}$ and $p \in$

$\{1, 2, 3, 4, 5, 6, 7, 8, 9, 10\}$. As we observe in Figure 2 (a - c), the IDSP performs robustly and insensitively on both the closed-set UDA and PDA tasks on a wide range of parameter values of p , λ and γ .

5.5 Effectiveness of Intra Domain Structure Preserving

We verify effectiveness of IDSP by inspecting the impacts of different structure preserving constraints. Specifically, we use no structure preserving (nP, i.e., $\gamma = 0$), conventional manifold structure preserving (CST), intra structure of both source and target domain (ST) and intra structure preserving of target domain (T, i.e., IDSP), whose results on the *Office-Home*, *Image-Clef* and *Office-31* are given in Figure 3. More details are given in Appendix D. It can be observed that the IDSP outperforms these baselines. From Figure 3, we easily find that the structure preserving can effectively enhance the adaptation ability of the classifier learned from the source domain, which confirms the superiority of model smoothness. Also, we can find that with more source structure information considered (i.e., ST and CST), the performance are reduced, especially in PDA. The reason is that the manifold structure across different domains may vary sharply (especially when the irrelevant categories exist) along with the domain shift, resulting in a negative transfer. The results illustrate the necessity to consider the intra domain structure preserving.

6 CONCLUSION

In this paper, considering the difficulty of the perfect alignment between domains while solving PDA, we endeavor to address the PDA by giving up domain alignment. To achieve it, a novel generalization error bound is first derived and then a theoretically-motivated PDA approach is proposed by enforcing intra domain structure preserving (IDSP). The experimental results demonstrate the effectiveness of the proposed IDSP, which confirms that IDSP scheme can be applicable to enhance the adaptation ability in solving PDA. This study also indicates that IDSP and conventional domain alignment can be complementary with each other in the UDA setting. In addition, it should be noted that IDSP naturally benefits the source-free UDA, since it only considers the target structure, which will be further studied

in our future work. In the end, we would like to emphasize that undoubtedly domain alignment remains important for domain adaptation. Thus, how to obtain harmless or perfect alignment with the guidance of model smoothness is still our next pursuit.

ACKNOWLEDGEMENT

The authors would like to thank Dr. Jingjing Gu and Dr. Yunyun Wang for the proofreading of this manuscript. This work is supported in part by the NSFC under Grant No. 62076124.

REFERENCES

- [1] S. Ben-David, J. Blitzer, K. Crammer, F. Pereira, *et al.*, "Analysis of representations for domain adaptation," *Advances in neural information processing systems*, vol. 19, p. 137, 2007.
- [2] S. Ben-David, J. Blitzer, K. Crammer, A. Kulesza, F. Pereira, and J. W. Vaughan, "A theory of learning from different domains," *Machine learning*, vol. 79, no. 1-2, pp. 151–175, 2010.
- [3] M. Sugiyama, T. Suzuki, S. Nakajima, H. Kashima, P. von Büna, and M. Kawanabe, "Direct importance estimation for covariate shift adaptation," *Annals of the Institute of Statistical Mathematics*, vol. 60, no. 4, pp. 699–746, 2008.
- [4] S. J. Pan, I. W. Tsang, J. T. Kwok, and Q. Yang, "Domain adaptation via transfer component analysis," *IEEE Transactions on Neural Networks*, vol. 22, no. 2, pp. 199–210, 2010.
- [5] B. Fernando, A. Habrard, M. Sebban, and T. Tuytelaars, "Unsupervised visual domain adaptation using subspace alignment," in *Proceedings of the IEEE international conference on computer vision*, pp. 2960–2967, 2013.
- [6] Y. Ganin and V. Lempitsky, "Unsupervised domain adaptation by backpropagation," in *International conference on machine learning*, pp. 1180–1189, 2015.
- [7] M. Long, J. Wang, G. Ding, S. J. Pan, and S. Y. Philip, "Adaptation regularization: A general framework for transfer learning," *IEEE Transactions on Knowledge and Data Engineering*, vol. 26, no. 5, pp. 1076–1089, 2013.
- [8] M. Baktashmotlagh, M. T. Harandi, B. C. Lovell, and M. Salzmann, "Unsupervised domain adaptation by domain invariant projection," in *Proceedings of the IEEE International Conference on Computer Vision*, pp. 769–776, 2013.
- [9] M. Belkin, P. Niyogi, and V. Sindhwani, "Manifold regularization: A geometric framework for learning from labeled and unlabeled examples," *Journal of machine learning research*, vol. 7, no. Nov, pp. 2399–2434, 2006.
- [10] J. Hoffman, E. Tzeng, T. Park, J.-Y. Zhu, P. Isola, K. Saenko, A. Efros, and T. Darrell, "Cycada: Cycle-consistent adversarial domain adaptation," in *International conference on machine learning*, pp. 1989–1998, PMLR, 2018.
- [11] Z. Cao, L. Ma, M. Long, and J. Wang, "Partial adversarial domain adaptation," in *Proceedings of the European Conference on Computer Vision (ECCV)*, pp. 135–150, 2018.
- [12] Z. Cao, K. You, M. Long, J. Wang, and Q. Yang, "Learning to transfer examples for partial domain adaptation," in *Proceedings of the IEEE Conference on Computer Vision and Pattern Recognition*, pp. 2985–2994, 2019.
- [13] T. Matsuura, K. Saito, and T. Harada, "Twins: Two weighted inconsistency-reduced networks for partial domain adaptation," *arXiv preprint arXiv:1812.07405*, 2018.
- [14] S. Li, C. H. Liu, Q. Lin, Q. Wen, L. Su, G. Huang, and Z. Ding, "Deep residual correction network for partial domain adaptation," *IEEE Transactions on Pattern Analysis and Machine Intelligence*, vol. 43, no. 7, pp. 2329–2344, 2021.
- [15] Y. Kim, S. Hong, S. Yang, S. Kang, Y. Jeon, and J. Kim, "Associative partial domain adaptation," *arXiv preprint arXiv:2008.03111*, 2020.
- [16] X. Liu, Z. Guo, S. Li, F. Xing, J. You, C. C. J. Kuo, G. E. Fakhri, and J. Woo, "Adversarial unsupervised domain adaptation with conditional and label shift: Infer, align and iterate," 2021.
- [17] J. Zhang, Z. Ding, W. Li, and P. Ogunbona, "Importance weighted adversarial nets for partial domain adaptation," in *Proceedings of the IEEE Conference on Computer Vision and Pattern Recognition*, pp. 8156–8164, 2018.
- [18] H. Liu, J. Wang, and M. Long, "Cycle self-training for domain adaptation," *arXiv preprint arXiv:2103.03571*, 2021.
- [19] W. Li and S. Chen, "Unsupervised domain adaptation with progressive adaptation of subspaces," *arXiv preprint arXiv:2009.00520*, 2020.
- [20] F. D. Johansson, D. Sontag, and R. Ranganath, "Support and invertibility in domain-invariant representations," in *The 22nd International Conference on Artificial Intelligence and Statistics*, pp. 527–536, PMLR, 2019.
- [21] H. Zhao, R. T. Des Combes, K. Zhang, and G. Gordon, "On learning invariant representations for domain adaptation," in *International Conference on Machine Learning*, pp. 7523–7532, PMLR, 2019.
- [22] V. Bouvier, P. Very, C. Chastagnol, M. Tami, and C. Hudelot, "Robust domain adaptation: Representations, weights and inductive bias," *arXiv preprint arXiv:2006.13629*, 2020.
- [23] B. Li, Y. Wang, T. Che, S. Zhang, S. Zhao, P. Xu, W. Zhou, Y. Bengio, and K. Keutzer, "Rethinking distributional matching based domain adaptation," *arXiv preprint arXiv:2006.13352*, 2020.
- [24] J. Wang, W. Feng, Y. Chen, H. Yu, M. Huang, and P. S. Yu, "Visual domain adaptation with manifold embedded distribution alignment," in *Proceedings of the 26th ACM international conference on Multimedia*, pp. 402–410, 2018.
- [25] V. Vapnik, *The nature of statistical learning theory*. Springer science & business media, 2013.
- [26] Y. Tsuboi, H. Kashima, S. Hido, S. Bickel, and M. Sugiyama, "Direct density ratio estimation for large-scale covariate shift adaptation," *Journal of Information Processing*, vol. 17, pp. 138–155, 2009.
- [27] J. Huang, A. Gretton, K. Borgwardt, B. Schölkopf, and A. J. Smola, "Correcting sample selection bias by unlabeled data," in *Advances in neural information processing systems*, pp. 601–608, 2007.
- [28] W. Zellinger, T. Grubinger, E. Lughofer, T. Natschlager, and S. Saminger-Platz, "Central moment discrepancy (cmd) for domain-invariant representation learning," *arXiv preprint arXiv:1702.08811*, 2017.
- [29] S. Si, D. Tao, and B. Geng, "Bregman divergence-based regularization for transfer subspace learning," *IEEE Transactions on Knowledge and Data Engineering*, vol. 22, no. 7, pp. 929–942, 2009.
- [30] M. Long, H. Zhu, J. Wang, and M. I. Jordan, "Deep transfer learning with joint adaptation networks," in *International conference on machine learning*, pp. 2208–2217, 2017.
- [31] K. Saito, K. Watanabe, Y. Ushiku, and T. Harada, "Maximum classifier discrepancy for unsupervised domain adaptation," in *Proceedings of the IEEE Conference on Computer Vision and Pattern Recognition*, pp. 3723–3732, 2018.
- [32] N. Courty, R. Flamary, and D. Tuia, "Domain adaptation with regularized optimal transport," in *Joint European Conference on Machine Learning and Knowledge Discovery in Databases*, pp. 274–289, Springer, 2014.
- [33] M. Long, Z. Cao, J. Wang, and M. I. Jordan, "Conditional adversarial domain adaptation," in *Advances in Neural Information Processing Systems*, pp. 1640–1650, 2018.
- [34] B. Sun, J. Feng, and K. Saenko, "Return of frustratingly easy domain adaptation," in *Thirtieth AAAI Conference on Artificial Intelligence*, pp. –, 2016.
- [35] Z. Cao, M. Long, J. Wang, and M. I. Jordan, "Partial transfer learning with selective adversarial networks," in *Proceedings of the IEEE Conference on Computer Vision and Pattern Recognition*, pp. 2724–2732, 2018.
- [36] C. Villani, *Optimal transport: old and new*, vol. 338. Springer, 2009.
- [37] M. Yi, L. Hou, J. Sun, L. Shang, X. Jiang, Q. Liu, and Z.-M. Ma, "Improved ood generalization via adversarial training and pre-training," *arXiv preprint arXiv:2105.11144*, 2021.
- [38] V. N. Vapnik, "An overview of statistical learning theory," *IEEE transactions on neural networks*, vol. 10, no. 5, pp. 988–999, 1999.
- [39] T. Chen, S. Kornblith, M. Norouzi, and G. Hinton, "A simple framework for contrastive learning of visual representations," in *International conference on machine learning*, pp. 1597–1607, PMLR, 2020.
- [40] K. He, H. Fan, Y. Wu, S. Xie, and R. Girshick, "Momentum contrast for unsupervised visual representation learning," in *Proceedings of the IEEE/CVF Conference on Computer Vision and Pattern Recognition*, pp. 9729–9738, 2020.
- [41] R. Rifkin, G. Yeo, T. Poggio, *et al.*, "Regularized least-squares classification," *Nato Science Series Sub Series III Computer and Systems Sciences*, vol. 190, pp. 131–154, 2003.

- [42] A. Rahimi, B. Recht, *et al.*, "Random features for large-scale kernel machines," in *NIPS*, vol. 3, p. 5, Citeseer, 2007.
- [43] K. Saenko, B. Kulis, M. Fritz, and T. Darrell, "Adapting visual category models to new domains," in *European conference on computer vision*, pp. 213–226, Springer, 2010.
- [44] H. Venkateswara, J. Eusebio, S. Chakraborty, and S. Panchanathan, "Deep hashing network for unsupervised domain adaptation," in *Proceedings of the IEEE Conference on Computer Vision and Pattern Recognition*, pp. 5018–5027, 2017.
- [45] K. He, X. Zhang, S. Ren, and J. Sun, "Deep residual learning for image recognition," in *Proceedings of the IEEE conference on computer vision and pattern recognition*, pp. 770–778, 2016.
- [46] M. Long, Y. Cao, J. Wang, and M. Jordan, "Learning transferable features with deep adaptation networks," in *International conference on machine learning*, pp. 97–105, 2015.
- [47] B. Gong, Y. Shi, F. Sha, and K. Grauman, "Geodesic flow kernel for unsupervised domain adaptation," in *2012 IEEE Conference on Computer Vision and Pattern Recognition*, pp. 2066–2073, IEEE, 2012.
- [48] M. Long, J. Wang, G. Ding, J. Sun, and P. S. Yu, "Transfer joint matching for unsupervised domain adaptation," in *Proceedings of the IEEE conference on computer vision and pattern recognition*, pp. 1410–1417, 2014.



Weikai Li received his B.S. degree in Information and Computing Science from Chongqing Jiaotong University in 2015. In 2018, he completed his M.S. degree in computer science and technique at Chongqing Jiaotong University. He is currently pursuing the Ph.D. degree with the College of Computer Science & Technology, Nanjing University of Aeronautics and Astronautics. His research interests include pattern recognition and machine learning..



Songcan Chen received his B.S. degree in mathematics from Hangzhou University (now merged into Zhejiang University) in 1983. In 1985, he completed his M.S. degree in computer applications at Shanghai Jiaotong University and then worked at NUAA in January 1986. There he received a Ph.D. degree in communication and information systems in 1997. Since 1998, as a full-time professor, he has been with the College of Computer Science & Technology at NUAA. His research interests include pattern recognition, machine learning and neural computing. He is also an IAPR Fellow.

APPENDIX A
GENERALIZATION ERROR

Theorem 1. Given two distributions \mathbb{P} and \mathbb{Q} , we denote $r = \max \|x_i - x_j\|_2$ where $\mathbf{W}_{ij} > 0$. If a model f is $2r$ -cover with ϵ smoothness over distributions \mathbb{P} and \mathbb{Q} , with probability at least $1 - \theta$, we have:

$$\begin{aligned} \mathcal{E}_{\mathbb{Q}}(f) &\leq \mathcal{E}_{\mathbb{P}}(f) + 2\epsilon + 2M TV(\mathbb{P}, \mathbb{Q}) \\ &\quad + M \sqrt{\frac{(2d)^{\frac{2\epsilon^2 D}{r^2} + 1} \log 2 + 2 \log(\frac{1}{\theta})}{m}} \\ &\quad + M \sqrt{\frac{(2d)^{\frac{2\epsilon^2 D}{r^2} + 1} \log 2 + 2 \log(\frac{1}{\theta})}{n}} \\ &\quad + M \sqrt{\frac{\log(1/\theta)}{2m}} \end{aligned} \quad (1)$$

Proof

Let $B_W(\mathbb{P}, r) = \{P : W_{\infty}(\mathbb{P}, P) \leq r\}$, where W_{∞} is the ∞ -th Wasserstein-distance [?]. Let $\mathbb{P}_r = \arg \min_{p \in B_W(\mathbb{P}, r)} \mathcal{E}_p(f)$ and $\mathbb{Q}_r = \arg \min_{q \in B_W(\mathbb{Q}, r)} \mathcal{E}_q(f)$

$$\begin{aligned} \mathcal{E}_{\mathbb{Q}}(f) &= \mathcal{E}_{\mathbb{Q}}(f) - \mathcal{E}_{\mathbb{Q}_r}(f) + \mathcal{E}_{\mathbb{Q}_r}(f) - \mathcal{E}_{\mathbb{P}}(f) + \mathcal{E}_{\mathbb{P}}(f) \\ &\leq \mathcal{E}_{\mathbb{P}}(f) + |\mathcal{E}_{\mathbb{Q}_r}(f) - \mathcal{E}_{\mathbb{Q}}(f)| \\ &\quad + |\mathcal{E}_{\mathbb{Q}_r}(f) - \mathcal{E}_{\mathbb{P}}(f)| \\ &\leq \mathcal{E}_{\mathbb{P}}(f) + |\mathcal{E}_{\mathbb{Q}_r}(f) - \mathcal{E}_{\mathbb{Q}}(f)| \\ &\quad + |\mathcal{E}_{\mathbb{Q}_r}(f) - \mathcal{E}_{\mathbb{P}_r}(f)| + |\mathcal{E}_{\mathbb{P}_r}(f) - \mathcal{E}_{\mathbb{P}}(f)| \end{aligned} \quad (2)$$

Then, according to the **Theorems 1 and 5** in recent study [?], we have

$$\begin{aligned} |\mathcal{E}_{\mathbb{P}_r}(f) - \mathcal{E}_{\mathbb{P}}(f)| &\leq \epsilon \\ &\quad + M \sqrt{\frac{(2d)^{\frac{2\epsilon^2 D}{r^2} + 1} \log 2 + 2 \log(\frac{1}{\theta})}{m}} \end{aligned} \quad (3)$$

$$\begin{aligned} |\mathcal{E}_{\mathbb{Q}_r}(f) - \mathcal{E}_{\mathbb{Q}}(f)| &\leq \epsilon \\ &\quad + M \sqrt{\frac{(2d)^{\frac{2\epsilon^2 D}{r^2} + 1} \log 2 + 2 \log(\frac{1}{\theta})}{n}} \end{aligned} \quad (4)$$

and

$$|\mathcal{E}_{\mathbb{Q}_r}(f) - \mathcal{E}_{\mathbb{P}_r}(f)| \leq 2M TV(\mathbb{P}, \mathbb{Q}) + M \sqrt{\frac{\log(1/\theta)}{2m}} \quad (5)$$

By plugging the Eqs. 3, 4 and 5 into Eq. 2, we have :

$$\begin{aligned} \mathcal{E}_{\mathbb{Q}}(f) &\leq \mathcal{E}_{\mathbb{P}}(f) + 2\epsilon + 2M TV(\mathbb{P}, \mathbb{Q}) \\ &\quad + M \sqrt{\frac{(2d)^{\frac{2\epsilon^2 D}{r^2} + 1} \log 2 + 2 \log(\frac{1}{\theta})}{m}} \\ &\quad + M \sqrt{\frac{(2d)^{\frac{2\epsilon^2 D}{r^2} + 1} \log 2 + 2 \log(\frac{1}{\theta})}{n}} \\ &\quad + M \sqrt{\frac{\log(1/\theta)}{2m}} \end{aligned} \quad (6)$$

Q.E.D

APPENDIX B
REPRESENTER THEOREM

Theorem 2. Representer Theorem: The parameter $\mathbf{W}^* = [\mathbf{w}_1^*, \dots, \mathbf{w}_h^*]$ for the optimized solution f of Eq.?? can be expressed in terms of the cross-domain labeled and unlabeled examples,

$$f(\mathbf{x}) = \sum_{i=1}^{n+m} \alpha_i K(\mathbf{x}_i, \mathbf{x}) \quad \text{and} \quad \mathbf{w} = \sum_{i=1}^{n+m} \alpha_i \phi(\mathbf{x}_i) \quad (7)$$

where K is a kernel induced by ϕ , α_i is a coefficient.

Proof It is easy to prove by contradiction. Denote $\text{span}(\phi(\mathbf{x}_i), 1 \leq i \leq n+m)$ as the linear space spanned by vectors $\phi(\mathbf{x}_i) : 1 \leq i \leq n+m$. Then, each \mathbf{W}_j can be expressed as

$$\mathbf{w}_j = \mathbf{w}_j^{\parallel} + \mathbf{w}_j^{\perp} \quad (8)$$

where \mathbf{w}_j^{\parallel} is the component along the linear space $\text{span}(\phi(\mathbf{x}_i), 1 \leq i \leq n+m)$ and \mathbf{w}_j^{\perp} is the component along its orthogonal complement space. Let the optimal solution

$$\mathbf{W}^* = \mathbf{W}^{*\parallel} + \mathbf{W}^{*\perp} \quad (9)$$

where $\mathbf{W}^{*\parallel} = [\mathbf{w}_1^{*\parallel}, \mathbf{w}_2^{*\parallel}, \dots, \mathbf{w}_m^{*\parallel}]$ and $\mathbf{W}^{*\perp} = [\mathbf{w}_1^{*\perp}, \mathbf{w}_2^{*\perp}, \dots, \mathbf{w}_m^{*\perp}]$. Then, we easily have $(\mathbf{W}^{*\perp})^T \mathbf{W}^{*\parallel} = \mathbf{0}$. We assume that $\mathbf{W}^{*\perp} \neq \mathbf{0}$, and denote $\mathcal{J}(\cdot)$ as the objective value of IDSP, then we have :

$$\begin{aligned} \mathcal{J}(\mathbf{W}^*) &= \sum_{i=1}^n (y_i - f(\mathbf{x}_i))^2 + \lambda \|\mathbf{f}\|_K^2 \\ &\quad + \gamma \sum_{i,j=1}^{n+m} f(\mathbf{x}_i) \mathbf{L}_{ij} f(\mathbf{x}_j) \\ &= \sum_{i=1}^n (y_i - \mathbf{w}^{*\top} \phi(\mathbf{x}_i))^2 + \lambda \text{tr}(\mathbf{w}^{*\top} \mathbf{w}^*) \\ &\quad + \gamma \sum_{i,j=1}^{n+m} \mathbf{w}^{*\top} \phi(\mathbf{x}_i) \mathbf{L}_{ij} \mathbf{w}^{*\top} \phi(\mathbf{x}_j) \\ &= \sum_{i=1}^n \left(y_i - \mathbf{w}^{*\parallel\top} \phi(\mathbf{x}_i) \right)^2 \\ &\quad + \lambda \left(\text{tr}(\mathbf{w}^{*\parallel\top} \mathbf{w}^{*\parallel}) + \text{tr}(\mathbf{w}^{*\perp\top} \mathbf{w}^{*\perp}) \right) \\ &\quad + \gamma \sum_{i,j=1}^{n+m} \mathbf{w}^{*\parallel\top} \phi(\mathbf{x}_i) \mathbf{L}_{ij} \mathbf{w}^{*\parallel\top} \phi(\mathbf{x}_j) \\ &\quad + \gamma \sum_{i,j=1}^{n+m} \mathbf{w}^{*\perp\top} \phi(\mathbf{x}_i) \mathbf{L}_{ij} \mathbf{w}^{*\perp\top} \phi(\mathbf{x}_j) \end{aligned} \quad (10)$$

while $\mathbf{W}^{*\perp} \neq \mathbf{0}$, and \mathbf{L} is the Laplacian matrix, we easily have $\mathcal{J}(\mathbf{w}^{*\parallel}) \leq \mathcal{J}(\mathbf{w}^*)$. Thus, $\mathbf{W}^{*\parallel}$ is more optimal than \mathbf{W}^* , which is contradictory with the fact. This yields the $\mathbf{W}^* = \mathbf{W}^{*\parallel}$.

Q.E.D

APPENDIX C

INTRA DOMAIN STRUCTURE PRESERVING WITH JOINT DOMAIN ADAPTATION FOR UDA

It should be noted that the risky of domain alignment tends to be lower in UDA. We further conduct experiments by adding an additional joint distribution adaptation (JDA) term [?]. The entire objective is given as follows:

$$f = \arg \min_{f \in \mathcal{H}_K} \sum_{i=1}^n (y_i - f(\mathbf{x}_i))^2 + \lambda \|f\|_K^2 + \gamma \sum_{i,j=1}^{n+m} f(\mathbf{x}_i) \mathbf{L}_{ij} f(\mathbf{x}_j) + \eta \mathcal{R}_{JDA}(f) \quad (11)$$

where $\mathcal{R}_{JDA}(f)$ is the JDA term, which is denoted as :

$$\mathcal{R}_{JDA}(f) = \left\| \frac{1}{n} \sum_{i=1}^n f(\mathbf{x}_i) - \frac{1}{m} \sum_{j=n+1}^{n+m} f(\mathbf{x}_j) \right\|_{\mathcal{H}}^2 + \left\| \frac{1}{n^{(c)}} \sum_{\mathbf{x}_i \in \mathcal{D}_s^{(c)}} f(\mathbf{x}_i) - \frac{1}{m^{(c)}} \sum_{\mathbf{x}_j \in \mathcal{D}_t^{(c)}} f(\mathbf{x}_j) \right\|_{\mathcal{H}}^2 \quad (12)$$

where $\mathcal{D}_s^{(c)} = \{\mathbf{x}_i : \mathbf{x}_i \in \mathcal{D}_s \wedge y(\mathbf{x}_i) = c\}$ is the set of the source data belonging to class c and $n^{(c)} = |\mathcal{D}_s^{(c)}|$. Correspondingly, $\mathcal{D}_t^{(c)} = \{\mathbf{x}_j : \mathbf{x}_j \in \mathcal{D}_t \wedge \hat{y}(\mathbf{x}_j) = c\}$, where $\hat{y}(\mathbf{x}_j)$ is the pseudo (predicted) label of \mathbf{x}_j and $m^{(c)} = |\mathcal{D}_t^{(c)}|$.

Learning Algorithm

Theorem 3. The minimizer of optimization problem 11 admits an expansion

$$f(\mathbf{x}) = \sum_{i=1}^{n+m} \alpha_i K(\mathbf{x}_i, \mathbf{x}) \quad \text{and} \quad \mathbf{w} = \sum_{i=1}^{n+m} \alpha_i \phi(\mathbf{x}_i) \quad (13)$$

where K is a kernel induced by ϕ , α_i is a coefficient. **Proof** The proof is similar to Theorem 2. Hence, we omit the proof for Theorem 3.

By incorporating Eq.13 into Eq. 11, we obtain the following objective:

$$\alpha = \arg \min_{\alpha \in \mathbb{R}^{n+m}} \left\| (\mathbf{Y} - \alpha^T \mathbf{K}) \mathbf{V} \right\|_F^2 + \text{tr}(\lambda \alpha^T \mathbf{K} \alpha + \alpha^T \mathbf{K} (\gamma \mathbf{L} + \eta \mathbf{M}) \mathbf{K} \alpha). \quad (14)$$

where \mathbf{V} is the label indicator matrix with $\mathbf{V}_{ii} = 1$ if $i \in \mathcal{D}_s$, otherwise $\mathbf{V}_{ii} = 0$. \mathbf{M} is the MMD matrix which can be computed as:

$$(M_C)_{ij} = \begin{cases} \frac{1}{n^{(c)} n^{(c)}}, & \mathbf{x}_i, \mathbf{x}_j \in \mathcal{D}_s^{(c)} \\ \frac{1}{m^{(c)} m^{(c)}}, & \mathbf{x}_i, \mathbf{x}_j \in \mathcal{D}_t^{(c)} \\ \frac{-1}{n^{(c)} m^{(c)}}, & \begin{cases} \mathbf{x}_i \in \mathcal{D}_s^{(c)}, \mathbf{x}_j \in \mathcal{D}_t^{(c)} \\ \mathbf{x}_j \in \mathcal{D}_s^{(c)}, \mathbf{x}_i \in \mathcal{D}_t^{(c)} \end{cases} \\ 0, & \text{otherwise} \end{cases} \quad (15)$$

Algorithm 1 Learning algorithm for PAS

Input:

n source labeled datasets $\mathcal{D}_s = \{\mathbf{x}_i^s, y_i\}_{i=1}^n$
 m target unlabeled datasets $\mathcal{D}_t = \{\mathbf{x}_i^s\}_{i=1}^m$
Hyper-parameters λ, γ, p and η ;

Output:

Predictive Classifier f

- 1: Initialize the Pseudo Label \hat{y}
- 2: Calculate the graph Laplacian \mathbf{L}
- 3: Construct kernel \mathbf{K} by a specific kernel function
- 4: **while** not converge **do**
- 5: Construct MMD matrix \mathbf{M} ;
- 6: Compute α ;
- 7: Update the Pseudo Label \hat{y}
- 8: **end while**
- 9: **Return** Classifier f .

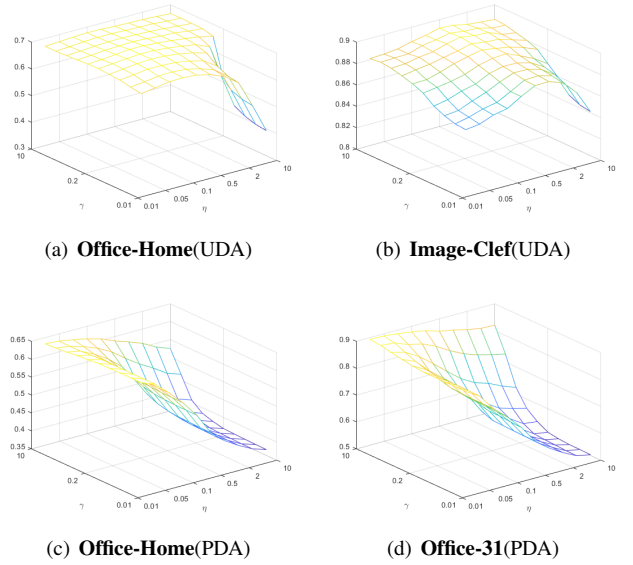


Fig. 1. classification accuracy w.r.t. η and γ , respectively

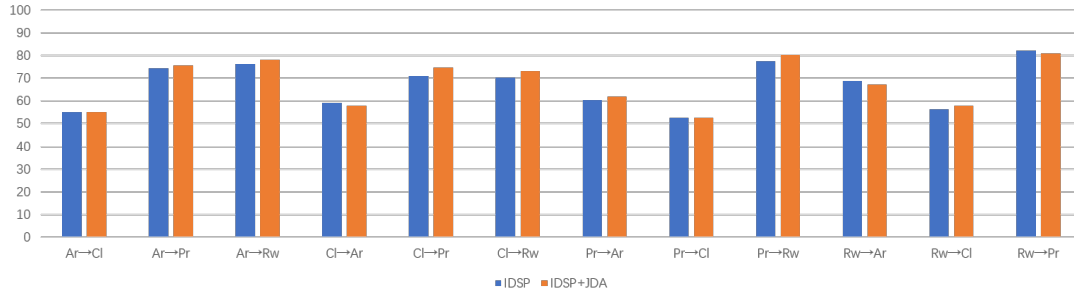
For clarity, we can also compute \mathbf{M}_0 with Eq. 15 if substituting $n^{(0)} = n, m^{(0)} = m, \mathcal{D}_s^{(0)} = \mathcal{D}_s, \mathcal{D}_t^{(0)} = \mathcal{D}_t$ Setting derivative of objective function as 0 leads to:

$$\alpha = ((\mathbf{V} + \gamma \mathbf{L} + \eta \mathbf{M}) \mathbf{K} + \lambda \mathbf{I})^{-1} \mathbf{V} \mathbf{Y}^T. \quad (16)$$

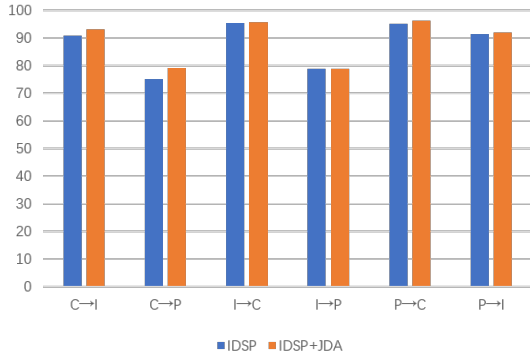
The learning algorithms are summarized in Algorithm 1.

Sensitivity Analysis

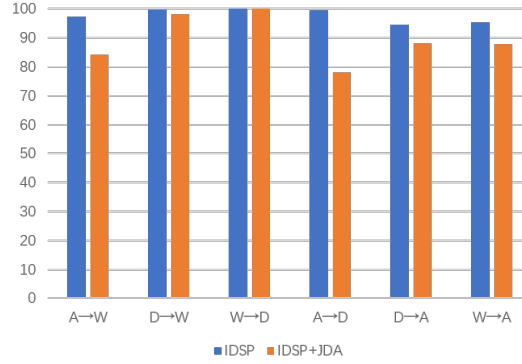
The proposed IDSP+JDA method involves one additional more hyper-parameters (i.e., η). To investigate the sensitivity of the smoothness and the domain alignment, we conduct experiments on *office-Home*, *Image-Clef* and *Office-31* datasets. Specifically, we ran IDSP by searching $\lambda \in \{0.01, 0.02, 0.05, 0.1, 0.2, 0.5, 1, 2, 5, 10\}$, $\eta \in \{0.01, 0.02, 0.05, 0.1, 0.2, 0.5, 1, 2, 5, 10\}$ with $\lambda = 0.1$ and



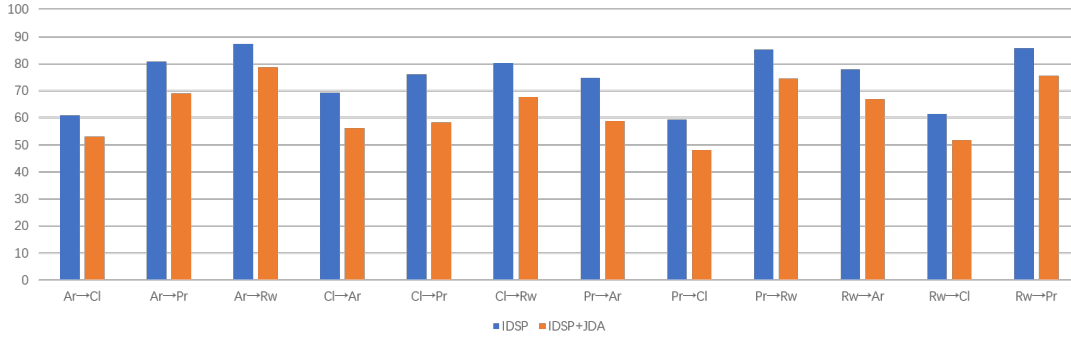
(a) Office-Home(UDA)



(b) Image-Clef(UDA)



(c) Office-31(PDA)



(d) Office-Home(PDA)

Fig. 2. classification accuracy of IDSP and IDSP+JDA

$p = 10$. As we observed in Figure 1, the IDSP performs robustly and insensitively on both the closed-set UDA on a wide range of parameter values of η and γ . To sum up, the performance of IDSP stays robust with a wide range of regularization parameter choice. They can be selected without knowledge in real applications. Further, the performance will be decrease with η increased in PDA. The results illustrates that domain alignment do not suit the PDA setting.

Classification Results

The classification results of IDSP and IDSP+JDA ($(\gamma = 2, \eta = 0.5$ for UDA and $\gamma = 10, \eta = 0.01$ for PDA) are given in Figure 2 and Table I. As we can observed in Figure 2 and Table I, with JDA incorporates in learning classier, the

TABLE I
ACCURACY(%) OF IDSP AND IDSP-JDA

DataSets	IDSP	IDSP-JDA
Office-Home(UDA)	67.0	68.0
Image-Clef(UDA)	87.9	89.3
Office-Home(PDA)	74.9	63.3
Office-31(PDA)	98.3	89.3

performance are increased in almost all tasks in the UDA setting. In contrast, the performance are significantly decreased in all tasks in the PDA setting. The results illustrate that the domain alignment may introduce negative transfer in PDA, since PDA do not satisfy the assumption of domain alignment.

In contrast, model smoothness can do well on both PDA and UDA settings.

APPENDIX D GRAPH CONSTRUCTION

In order to demonstrate the effectiveness of the proposed Intra Domain Structure Preserving, we perform an ablation study by learning a classifier with different structure preserving constraints. Specifically, we use no structure preserving (nP, i.e., $\gamma = 0$), manifold structure preserving of source and target domain (CST), intra structure of both source and target domain (ST) and intra structure preserving of target domain (T). The pair-wise affinity matrix $\hat{\mathbf{G}}^{(T)}$ of the graph can be formulated as follows:

$$\mathbf{G}_{ij}^{(T)} = \begin{cases} \hat{\mathbf{G}}_{ij}, & \mathbf{x}_i \text{ and } \mathbf{x}_j \in \mathcal{D}_t \\ 0, & \text{otherwise} \end{cases} \quad (17)$$

The pair-wise affinity matrix $\hat{\mathbf{G}}^{(ST)}$ of the graph can be formulated as follows:

$$\mathbf{G}_{ij}^{(ST)} = \begin{cases} \hat{\mathbf{G}}_{ij}, & (\mathbf{x}_i, \mathbf{x}_j) \in \mathcal{D}_t \text{ or } (\mathbf{x}_i, \mathbf{x}_j) \in \mathcal{D}_s \\ 0, & \text{otherwise} \end{cases} \quad (18)$$

The pair-wise affinity matrix $\hat{\mathbf{G}}^{(CST)}$ of the graph can be formulated as follows:

$$\mathbf{G}_{ij}^{(ST)} = \hat{\mathbf{G}}_{ij} \quad (19)$$